Journal of Catalysis **187,** 410–418 (1999)
Article ID jcat.1999.2626, available online at http://www.idealibrary.com on IDEAL®

Oxidative Dehydrogenation of Propane on $Ni_xMg_{1-x}Al_2O_4$ and $NiCr_2O_4$ Spinels

Jerzy Słoczyński,* Jacek Ziółkowski,* Barbara Grzybowska,*,[1] Ryszard Grabowski,* Dariusz Jachewicz,* Krzysztof Wcisło,* and Leon Gengembre†

*Institute of Catalysis and Surface Chemistry, Polish Academy of Sciences, ul. Niezapominajek 30-239 Kraków, Poland; and †Laboratoire de Catalyse Hétérogène, URA CNRS 402, Université des Sciences et Technologies de Lille, 59 655 Villeneuve d'Ascq Cédex, France

Received March 16, 1999; revised July 5, 1999; accepted July 6, 1999

The $Ni_xMg_{1-x}Al_2O_4$, $NiCr_2O_4$, and $MgCr_2O_4$ spinels have been synthesized, characterized with the XRD and XPS methods, and tested in the oxidative dehydrogenation of propane. The crystallochemical model of solid surfaces, CMSS, has been used to calculate the oxygen cation's bond energies in the spinels. For the NiMgAl spinels the activity and selectivity to propene increase with the increase in the Ni content. The Ni ions surrounded by oxygen in the spinel structure are proposed as active centers for oxidative dehydrogenation to propene. The NiCr spinel is more active but less selective than the NiMgAl spinels; the difference in catalytic behavior has been ascribed to different coordination of Ni ions in the two groups of the spinels and to the lower oxygen cation's bond energy in the NiCr spinel.

Key Words: **oxidative dehydrogenation of propane; nickel-chrom spinels; nickel-magnesium-aluminium spinels.**

INTRODUCTION

Nickel-containing systems have been found in the past decade to be active and selective catalysts in oxidative dehydrogenation (ODH) of alkanes, a reaction proposed recently as an alternative to classical dehydrogenation for the production of cheap olefins. Nickel molybdate has been reported as efficient in the ODH of propane (1–4), whereas nickel phosphate $Ni_2P_2O_7$ (5, 6) and NiO dispersed on different supports (7) are shown to be promising catalysts in the respective reaction of isobutane.

There is practically no information about the structure of the active centers and the role of the environment of nickel ions in the ODH reactions. In an attempt to approach this problem in the present work the catalytic performance in the ODH of propane has been studied for the NiMgAl and NiCr spinels characterized, respectively, by octa- and tetrahedral coordination of Ni ions in the Ni–O polyhedra.

The series of the $Ni_xMg_{1-x}Al_2O_4$ spinels of different Ni content and the $NiCr_2O_4$ and $MgCr_2O_4$ spinels were synthesized. Their structure and composition, both in the bulk and on the surface, have been verified with XRD and XPS techniques, respectively. The crystallochemical model of solid surfaces (CMSS) (8–11), described briefly in the next paragraphs, has been also applied to evaluate the oxygen binding energies in different coordination of the ions, both in the bulk and on the surface of the studied systems.

EXPERIMENTAL

Preparation of the Catalysts

The $Ni_xMg_{1-x}Al_2O_4$ ($0 \le x \le 1$) and $MgCr_2O_4$ spinels were prepared with the citrate method using solutions of nitrates of the respective metals (0.5–2 M) and 2 M citric acid as precursors. All the starting materials were of high purity (at least proanalysis grade).

The desired amounts of the nitrates were introduced drop-wise to the solution of citric acid in 2–3% excess with respect to the stoichiometry of the given citrates. The solutions were evaporated in a vacuum rotary evaporator at 363 K for 3 h. The final drying was effectuated at 673 K for 6 h. The vitrous precursors thus obtained were carefully ground and calcined in an alundum crucible in a stream of air at 823 K for 24 h and then again in air at 1173 K for 144 h. In the course of the last calcination the samples were cooled down every 48 h, ground in a mortar, and pulverized in an ultrasonic disperser. The $NiCr_2O_4$ spinel was obtained with a coprecipitation method. The NH_3aq (14%) was added step-wise to a solution of nickel and chromium nitrates kept at 353 K under continous stirring till pH $\approx$ 6.5 was reached. The precipitate was aged on a water bath for 2 h, filtered, washed with water, and dried at 373 K. The coprecipitated Ni [II] and Cr [III] hydroxides were decomposed in air at 773 K for 5 h; the sample was then ground, tableted, and calcined at 1173 for 40 h. The specific surface areas of the preparations are given in Table 5.

[1] To whom correspondence should be addressed.

0021-9517/99 $30.00

XPS

XPS spectra of the samples were recorded with a Leybold Heraeus LHS 10 spectrometer using an Al $K\alpha$ X-ray source with incitent radiation at 1486.6 eV. The base pressure was 10^{-8} T. The surface stoichiometry was calculated from the intensity ratios I_A/I_B of the elements using the formula

$$I_A/I_B = \sigma_A/\sigma_B \cdot \left(E_A^{\mathrm{kin}}/E_B^{\mathrm{kin}}\right)^{1.77} n_A/n_B, \qquad [1]$$

where σ are the cross-sections taken from (12) and n_A and n_B are the numbers of atoms on the surface.

XRD

The XRD diffractograms were recorded with a DRON-2 diffractometer (Cu $K\alpha$, a Ni filter, Al as an internal standard) equipped with a DAS interface. The spectra were interpreted using the SMOK (Elector Co., Kraków) and LATCON (CERN library) programs. The simulation of diffractograms of the spinels of different inversion degree was performed with the use of Rietveld's program DBWS-9006 PC (A. Sakthivel and R. A. Young, Atlanta).

Catalytic Activity Measurements

The activity of the catalysts in oxidative dehydrogenation of propane was measured in a fixed bed flow apparatus in the temperature range 673–773 K. A stainless steel reactor (120 mm long, internal diameter 13 mm) was coupled directly to a series of gas chromatographs. Propene and carbon dioxide were found to be main reaction products and small amounts of carbon monoxide were also observed. The amounts of the degradation, C_2 products, and oxygenates (acrolein and acrylic acids) were below 1% of the total amount of products. The reaction mixture contained 7.1 vol.% of propane in air. The flow rate of the reaction mixture was controlled with a flow meter type ERG-IMKZ. One to 2 g samples of a catalyst of grain size 0.63–1 mm were used. It has been checked in the preliminary measurements in which the mass and the grain size of a catalyst sample were varied, that under these conditions the transport phenomena do not limit the reaction rate. For each sample the activity measured on increasing and decreasing the temperature was reproducible within the limits of experimental error (5%). A sample was kept at each reaction temperature for about 20 h; no deactivation of the catalysts was observed during this period. The kinetic measurements were performed measuring at each temperature concentrations of unreacted propane and of reaction products as a function of a contact time τ. The latter was varied between 0.1 and 3 s by changing the flow rate of the reaction mixture. The values of the total conversion of propane did not exceed 30%. The carbon balance for conversions higher than about 10% was better than $97 \pm 2\%$. At lower conversions the balance was poorer and hence the selectivities to different products were calculated from the formula $S_i = c_i/\sum c_i$, where c_i are concentrations of products i. The total conversion values X_{p} were calculated as

$$X_{\mathrm{p}} = \frac{c_{\mathrm{p}}^0 - c_{\mathrm{p}}}{c_{\mathrm{p}}^0}, \qquad [2]$$

where c_{p}^0 and c_{p} are the concentrations of propane at the inlet and outlet of the reactor, respectively.

RESULTS AND DISCUSSION

XPS

Figure 1 shows the XPS Ni 2p spectra for the samples of $NiAl_2O_4$, and $NiCr_2O_4$. The spectra of other $Ni_xMg_{1-x}Al_2O_4$ samples resemble that of the $NiAl_2O_4$ spectrum. Table 1 lists the binding energies (BE) and the full width at half-maximum (FWHM) of Ni 2p, O 1s, Al 2p, Mg 1s, and Cr 2p levels in the studied samples. The shift between the Ni $2p_{3/2}$ signal and its satellite, ΔE_{sat}, and the ratio of intensities (the peak heights) of the satellite to principal peaks of the Ni $2p_{3/2}$ spectrum $I_{\mathrm{sat}}/I_{\mathrm{p}}$ are also reported. The error in the estimation of the surface content of a given element is $\pm 5\%$, the sum of positive (Ni^{2+}, Mg^{2+}, Al^{3+}, Cr^{3+}) and negative (O^{2-}) charges is balanced within $\pm 4\%$. Following the literature data (13–16) the values of BE for the Ni 2p level and of the satellite shift ΔE as well as the $I_{\mathrm{sat}}/I_{\mathrm{p}}$ ratio permit identification of the Ni ions as divalent in octahedral ($NiAl_2O_4$ and $Ni_xMg_{1-x}Al_2O_4$) and tetrahedral ($NiCr_2O_4$) environments. The last column gives the surface stoichiometry of the samples calculated from the XPS data.

As seen the surface stoichiometry of the samples is close to that of the bulk of the samples assumed at the preparation of the respective spinels.

XRD

All of the prepared samples gave diffractograms characteristic of pure spinels with sharp, easily indexed reflexions. The values of lattice constants were in good agreement with the literature data (17) or, in the case of $Ni_xMg_{1-x}Al_2O_4$, with those obtained by the interpolation.

The MgNiAl spinels showed a cubic X-ray pattern while in the case of $NiCr_2O_4$ tetragonal distortion connected with the Jahn–Teller effect was observed. Tetragonal form transforms into cubic at 310–330 K (18, 19).

If we describe $A^{\mathrm{II}}B^{\mathrm{III}}O_4$ spinels by the general formulae accounting for the tetrahedral ( ) and octahedral [ ] distribution of A and B cations we have: $(A)[B_2]O_4$ (normal spinel), $(B)[AB]O_4$ (inversed spinel), and $(A_{1-z}B_z)[A_zB_{2-z}]O_4$ (mixed spinel), where z is the inversion degree.

Figure 2a presents a typical diffractogram of the $NiAl_2O_4$ spinel, whereas in Figs. 2b and 2c, the diffractograms are simulated with the DBWS program for $z = 1$ and 0,

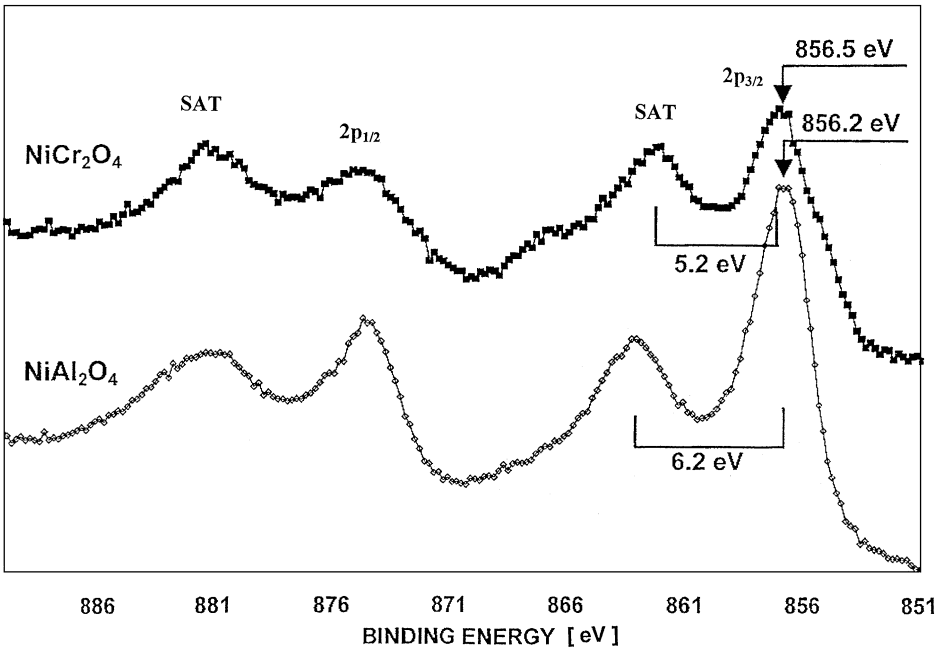

FIG. 1. XPS spectra of $NiAl_2O_4$ and $NiCr_2O_4$ in the Ni 2p region.

respectively. It is seen that the diffractogram of $NiAl_2O_4$ strongly resembles the simulated pattern of the inversed spinel.

Table 2 lists lattice constants calculated from the experimental data, packing coefficient of the oxygen ions, *u* (literature or interpolated data), and the distribution of cations between the tetra- and octahedral positions determined with the Bertaut–Greenwald method (20–21). The method consists of comparison of the ratios of experimental intensities of reflexions *I* (400)/*I* (220) and *I* (400)/*I* (224) with the theoretical values simulated with the DBWS-9006 PC program. For most of the studied samples the coefficients ( )/[ ] were determined with the accuracy 0.01–0.04; for the NiCr sample it was lower, amounting to 0.1. The results

TABLE 1

XPS Data for Nickel Spinels

Spinel	BE, eV ⟨FWHM⟩ Ni $2p_{3/2}$	BE, eV ⟨FWHM⟩ O_{1s}	Me	Ni (ΔE_{sat})	I_s/I_p	Surface stoichiometry
$NiAl_2O_4$	856.2 ⟨3.2⟩	531.1 ⟨2.5⟩	Al 2p. 74.2 ⟨≈2.4⟩	6.2	0.51	$NiAl_2O_{4.1}$
$Ni_{0.1}Mg_{0.9}Al_2O_4$	856.4 ⟨3.3⟩	531.2 ⟨2.9⟩	Mg 1s 1304.2 ⟨2.7⟩ Al 2p. 74.2 ⟨≈2.3⟩	6.3	0.51	$Ni_{0.14}Mg_1Al_2O_{4.1}$
$Ni_{0.5}Mg_{0.5}Al_2O_4$	856.2 ⟨3.2⟩	531.1 ⟨2.7⟩	Mg 1s 1304.0 ⟨2.5⟩ Al 2p. 74.2 ⟨≈2.4⟩	6.3	0.49	$Ni_{0.5}Mg_{0.58}Al_{1.85}O_4$
$NiCr_2O_4$	856.5 ⟨≈4.3⟩	530.2 ⟨1.9⟩	Cr $2p_{3/2}$ 576.7 ⟨3.5⟩	5.2	0.74	$NiCr_{2.2}O_{4.1}$

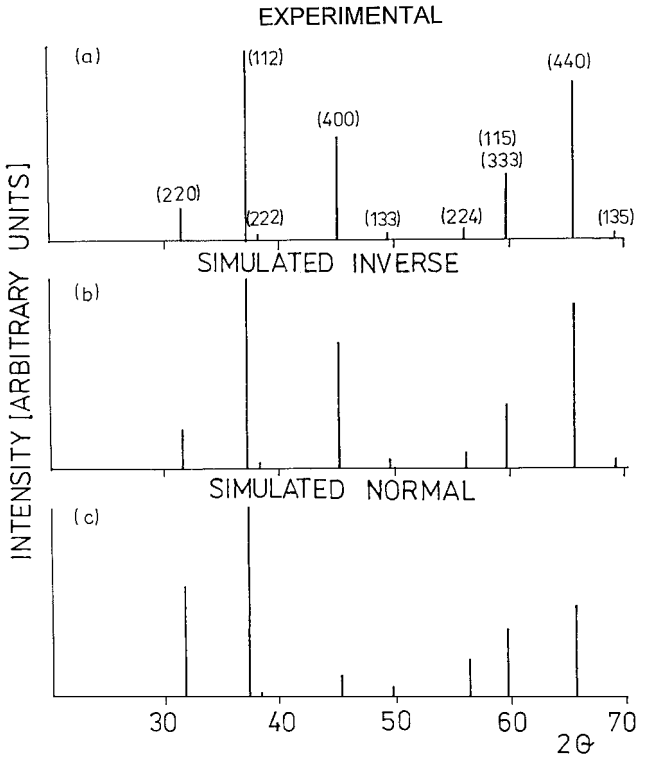

FIG. 2. Diffractograms of $NiAl_2O_4$ spinel. Experimental (a), simulated with the DBWS program; inverse spinel (b); normal spinel (c).

confirm the structure of the spinels reported in the literature: NiAl preparation is pure inverse spinel and MgCr and NiCr are normal spinels, whereas the MgNiAl preparations are almost totally inverse spinels.

Oxygen Cations and Cation–Oxygen Binding Energies

Table 3 gives the values of the oxygen cation's binding energies ΣE in $NiAl_2O_4$, $NiCr_2O_4$, and $MgCr_2O_4$, calculated for different coordinations in the bulk and on the surface of the spinels with the CMSS (8–11). The model is based on a new empirical correlation proposed in (8) between the bond strength, *s*, defined first by Pauling as the valence of a cation divided by its coordination number in a crystal, and the bond length *R*. Multiplication of *s* derived from this correlation by a coefficient *J* normalized to the enthalpy of atomization of a simple oxide of a considered cation gives the bond energy *E* expressed in the energy unit as a function of *R* (9). The bond energy will then depend on structural factors (reflected in the bond length, *R*, different for different coordinations, not necessarily symmetrical) and on intrinsic properties of a cation included in the value of *J*. It should be noted that the coefficient *J* involves the enthalpy of atomization of an oxide and not the lattice energy which is the formation energy of the oxide from ions. The values of *E* are only approximate since the model does not take into account the long-range coulombic interactions as was done with more sophisticated methods; see, for example, Refs. (22, 23). In spite of these shortcomings the model has been successfully applied to explain the catalytic properties of several oxide catalysts in oxidation reactions, as a function of the calculated Me–O bond energies (10, 24, 25). In calculations of the oxide surface, the sum of energies of local missing bonds ΣE_c per surface unit cell area has been assumed to be the surface energy, E_{surf} (11). The surface slices are selected according to the minimum of E_{surf}. In accordance with E_{surf} the equilibrium shape of the grains has been determined with the Curie–Wulff construction and the impact of various (hkl) faces to the external surface has been calculated (11). The rigid surface model neglecting the surface relaxation phenomena has been adapted in the calculations. It is, however, assumed that a molecule reacting on the surface plays the role of an additional ligand neutralizing (absorbing) the local relaxation energy (10, 11).

In the structure of spinels each oxygen ion coordinates four cations, one of which is tetra- and three octacoordinated: $1 \times O - (\ ) + 3 \times O - [\ ]$. ΣE is a sum of the

TABLE 2

Structural Data of the NiMgAl, NiCr, and MgCr Spinels

Spinel	a (Å)[a]	u[b]	Cation distribution[c]	
$MgAl_2O_4$	8.0833(10)	0.2624	$(Mg_{0.77}Al_{0.23})$	$[Mg_{0.23}Al_{1.77}]$
$Mg_{0.9}Ni_{0.1}Al_2O_4$	8.0790(10)	0.2618	$(Mg_{0.90}Al_{0.10})$	$[Ni_{0.10}Al_{1.90}]$
$Mg_{0.5}Ni_{0.5}Al_2O_4$	8.0617(13)	0.2594	$(Mg_{0.50}Ni_{0.03}Al_{0.47})$	$[Ni_{0.47}Al_{1.53}]$
$NiAl_2O_4$	8.0426(17)	0.2560	$(Al_{1.00})$	$[Ni_{1.0}Al_{1.00}]$
$MgCr_2O_4$	8.3374(25)	0.2612	$(Mg_{1.00})$	$[Cr_{2.00}]$
$NiCr_2O_4$	$a = 8.2545(10)$			
	$c = 8.4269(15)$		$(Ni_{1.00})$[d]	$[Cr_{2.00}]$[d]

[a] Experimental.
[b] Literature or interpolated data.
[c] Determined with the Bertaut–Greenwald method (typical error for the coefficient of the predominating ion in the indicated position is 5%).
[d] According to (17).

TABLE 3

Oxygen Cation's and Metal–Oxygen Binding Energies ΣE and E(Me-O) (kcal mol^{-1}) in Various Environments in the Bulk and at the Surface of NiAl, NiCr and MgCr Spinels

$NiAl_2O_4$			$NiCr_2O_4$			$MgCr_2O_4$		
E(Me–O)			E(Me–O)			E(Me–O)		
Ni Oc	Al Td	Al Oc	Ni Td	Ni Oc	Cr Oc	Mg Td	Mg Oc	Cr Oc
36.60	91.58	61.05	54.90	36.60	53.30	59.55	39.70	53.30
Coordination		ΣE	Coordination		ΣE	Coordination		ΣE
Bulk			Bulk			Bulk		
(Al) [AlAlAl]		274.73	(Ni) [CrCrCr]		214.80	(Mg) [CrCrCr]		219.45
(Al) [AlAlNi]		250.28						
(Al) [AlNiNi]		225.83						
(Al) [NiNiNi]		201.38						
Surface			Surface			Surface		
−1 Td			−1 Td			−1 Td		
[AlAlAl]		183.15	[CrCrCr]		159.90**	[CrCrCr]		159.90**
[AlAlNi]		158.70**						
[AlNiNi]		134.25**						
−1 Oc			−1 Oc			−1 Oc		
(Al) [AlAl]		213.68	(Ni) [CrCr]		161.50**	(Mg) [CrCr]		166.15**
(Al) [AlNi]		189.23**						
(Al) [NiNi]		164.78						
−2 Oc			−2 Oc			−2 Oc		
(Al) [Al]		152.63**	(Ni) [Cr]		108.20**	(Mg) [Cr]		112.82**
(Al) [Ni]		128.18**						

Note. Td, tetrahedral sites; Oc, octahedral sites; **, the most probable surface sites.

energies of all O-cation bonds existing in a given oxygen coordination, which determines the ability of abstraction of an oxygen ion from the catalysts.

It has been shown in previous works (24, 26) that the most frequently exposed faces of the spinels (100), (110), and (111) exhibit unsaturated oxygen atoms of the following coordinations:

$$3 \times O - [\,] \; (=-1\,Td)$$
$$1 \times O - (\,) + 2 \times O - [\,] \; (=-1\,Oc)$$
$$1 \times O - (\,) + 1 \times O - (\,) \; (=-2\,Oc).$$

On the spinel surface one tetrahedral (−1 Td) or one octahedral (−1 Oc) or two octahedrals (−2 Oc) are missing with respect to the bulk. The most probable surface coordinations of oxygen are marked with **. Table 3 provides also the binding energies, E (Me–O) for the Mg–O, Ni–O, and Cr–O bonds in tetrahedral (Td) and octahedral (Oc) sites.

As seen from the table, for the same type of environment of the oxygen ions the values of ΣE both in the bulk and on the surface of the spinels are distinctly higher for $NiAl_2O_4$ than for the Cr-containing compounds. This is due to the higher Al–O binding energy as compared with that of Mg–O or Ni–O bonds. For the two Cr-containing compounds, oxygen is more strongly bound in $MgCr_2O_4$ than in $NiCr_2O_4$, which may arise from the stronger Mg–O bond as compared with the Ni–O bond.

Catalytic Performance and Its Relation to the Composition and Structure of the Catalysts

Figure 3 presents the changes of the selectivities to the main reaction products, propene and CO_2, with total propane conversion at 723 K for the NiMgAl spinels. The selectivity to propene increases and that to CO_2 decreases with the increase in the Ni content. In Fig. 4 the curves of the propene selectivity vs conversion for the NiAl and MgAl spinels are compared with those for the Cr-containing compounds and with the data for pure oxides Al_2O_3 and MgO. As seen from Fig. 4 the NiAl spinel is, at comparable conversions, much more selective in the propene formation than $NiCr_2O_4$. The selectivities to propene for $NiAl_2O_4$ are comparable to those reported for the best catalysts in the ODH of propane, i.e., $NiMoO_4$ (1–4) and V–Mg–O (27–29) systems.

The MgAl and MgCr spinels, MgO and Al_2O_3, show low activity in the propane–oxygen reaction, their selectivities to propene being considerably lower than those for $NiAl_2O_4$ and higher than the selectivities for $NiCr_2O_4$.

The decrease of the selectivity to propene accompanied by the increase in the selectivity to CO_2 indicates the

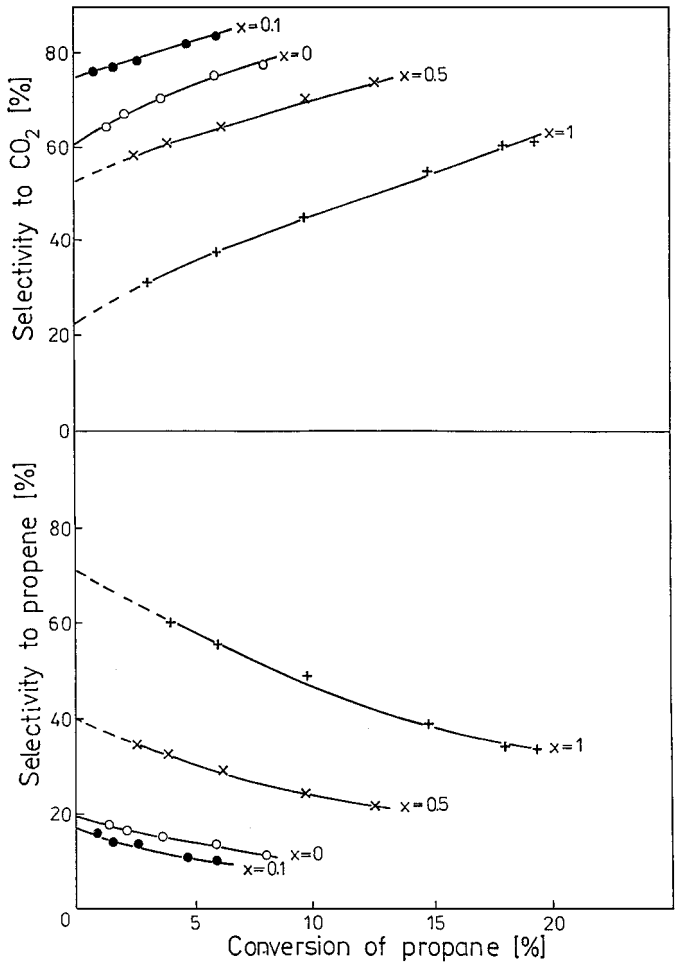

FIG. 3. Selectivity to main products of the $C_3H_8 + O_2$ reactions as a function of propane conversion for $Ni_xMg_{1-x}Al_2O_4$ spinels.

consecutive route of the reaction, in which propene formed in the primary reaction is further oxidized to CO_x. The fact that selectivities to propene extrapolated to 0th conversion are considerably lower than 100% suggests, moreover, that a fraction of carbon oxides is formed also by a route parallel to propene formation. The propane–oxygen reactions on the studied catalysts can be hence described by the following network:

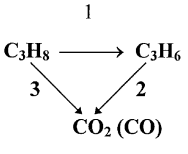

[3]

In Fig. 5 the propane conversion at 723 K is plotted as a function of contact time τ for the NiMgAl spinels of different Ni content. The curves are calculated according to the equation of the first order with respect to propane; the points represent the experimental data. The correlation coefficients are comprised between 0.952 and 0.975. The first order with respect to propane can be then used as a first approximation in description of the reaction network. The first order with respect to propane has been also reported for the ODH propane on other catalysts, e.g., V_2O_5/TiO_2 (30–32) or CoNi molybdates (33). In the same works (31–33) the 0th order with respect to oxygen has been found. Our data on reduction with propane and reoxidation with gaseous oxygen of the V_2O_5/TiO_2 pure and alkali promoted catalysts (34) indicate, moreover, that the surface reoxidation rate is considerably higher than that of the reduction. It seems justified then to assume that in the present measurements, in which an excess of oxygen in the reaction is used, the reaction is of the first order with respect to propane and is independent of the oxygen pressure. The first order with respect to propene in step 2 is also assumed. With these assumptions the expressions for the rates of different steps shown in Scheme 3 are given by

$$-\frac{dc_p}{d\tau} = k_p c_p, \quad \frac{dc_\pi}{d\tau} = k_1 c_p - k_2 c_\pi \qquad [4]$$

$$\frac{1}{3}\frac{dc_{COx}}{d\tau} = k_3 c_p + k_2 c_\pi \qquad [5]$$

where $k_p = k_1 + k_3$, c_p, and c_π are concentrations of propane and propene, respectively.

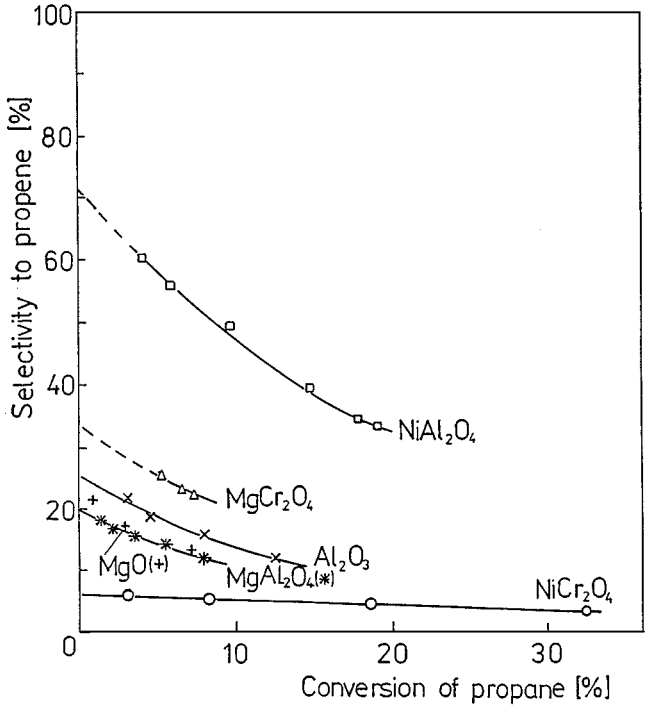

FIG. 4. Comparison of selectivity vs conversion curves for Ni(Mg)Al and Ni(Mg)Cr spinels.

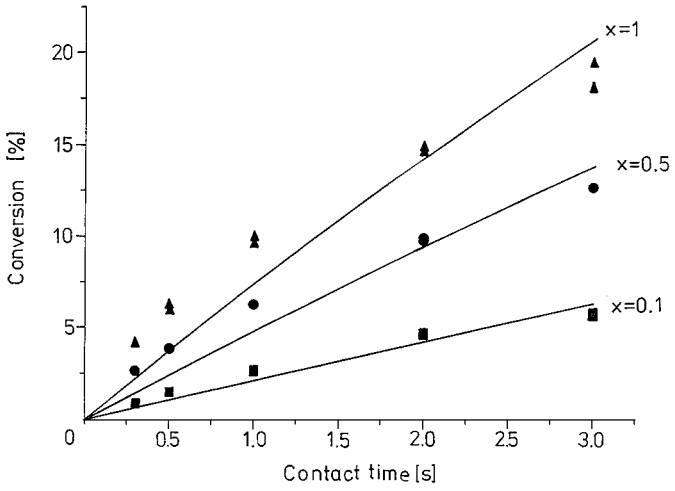

FIG. 5. Propane conversion as a function of contact time for $Ni_xMg_{1-x}Al_2O_4$ spinels. Reaction temperature, 723 K.

The solutions of the above equations give the following expressions for conversion and selectivities:

$$X_p = 1 - \exp(-k_p\tau), \qquad [6]$$

$$S_\pi = \frac{k_1}{k_2 - k_p}\,\frac{\exp(-k_p\tau) - \exp(-k_2\tau)}{1 - \exp(-k_p\tau)}$$

$$S_{COx} = \frac{k_3}{k_p} + \frac{k_1k_2}{k_2 - k_p}\left[\frac{1}{k_p} - \frac{1}{k_2}\,\frac{1 - \exp(-k_2\tau)}{1 - \exp(-k_p\tau)}\right], \qquad [7]$$

$$S_{COx} = 1 - S_\pi.$$

The rate constants k_1, k_2, k_3 were calculated by a standard nonlinear regression method with the Sigma-plot program (Jandel Scientific).

Table 4 lists the values of the specific rates of reactions 1, 2, and 3 obtained using the calculated values of k_i ($i = 1, 2, 3$) for the propane and propene initial content of 7.1 vol.% for all the studied spinels. The activation energies of steps 1, 2, and 3 for the $Ni_xMg_{1-x}Al_2O_4$ spinels are also given.

Generally, the rates of the three reactions are higher for the Cr-containing spinels as compared with those containing Al. The Mg spinels (MgAl and MgCr preparations) have much lower activity in the three reactions than the respective Ni spinels, suggesting that the active centers in the propane–oxygen reactions in NiMgAl and NiCr systems involve Ni ions. By analogy to oxidation reactions of other hydrocarbons (35) a Ni^{2+}–O^{2-} couple can be envisaged as an active center for the propane reactions, the oxygen ions participating in abstraction of a hydrogen from a hydrocarbon molecule and/or in incorporation into the products. Ni ions on the other hand facilitate the activation of the C–H bond and the electron transfer.

$MgCr_2O_4$ is considerably more active than $MgAl_2O_4$, which indicates that Cr ions can also catalyze the reactions under consideration, though to a smaller extent than Ni. The activity of Cr in chromium oxide dispersed on supports in the ODH of propane and isobutane has been in fact observed in earlier works (36–39).

Another general observation is that the rates of oxidation of propene to CO_x (step 2) are considerably higher than those of the propene formation from propane. This phenomenon, observed previously for other catalytic systems (30–32), has been explained by lower energy of allylic C–H bond in a propene molecule as compared with that of the parafinic bonds in propane.

For the $Ni_xMg_{1-x}Al_2O_4$ spinels at all the reaction temperatures the specific rate of step 1 increases with the increase in the Ni content, x, confirming that the Ni ions are involved in active centers for oxidative dehydrogenation of propane to propene. The rates of steps 2 and 3 show, on the other hand, a maximum at $x = 0.5$ (except for step 2 at the highest reaction temperature 773 K). This suggests that other centers beside Ni ions may contribute to total oxidation reactions and/or different surface complexes of adsorbed hydrocarbons are responsible for selective and

TABLE 4

Catalytic Activity of the Ni Contained Spinels in ODH of Propane

Catalyst	Specific surface area ($m^2\,g^{-1}$)	Specific catalytic activity × 10^3 μmol C_3H_8 (C_3H_6) $s^{-1}\,m^{-2}$									Activation energy (kJ mol^{-1})		
		$C_3H_8 \rightarrow C_3H_6$ Temp., K			$C_3H_8 \rightarrow CO_x$ Temp., K			$C_3H_6 \rightarrow CO_x$ Temp., K					
		673	723	773	673	723	773	673	723	773	E_1	E_3	E_2
$MgAl_2O_4$	20.7	0	0.26	0.90	—	2.86	7.56	—	39	47	115	91	17
$Ni_{0.1}Mg_{0.9}Al_2O_4$	12.0	0.21	0.79	2.47	1.33	4.23	11.46	61	79	99	107	94	25
$Ni_{0.5}Mg_{0.5}Al_2O_4$	7.3	1.58	5.86	12.14	3.59	10.37	17.6	92	135	188	89	86	31
$NiAl_2O_4$	9.15	5.20	12.15	25.42	3.22	6.93	13.47	73	122	203	69	62	43
$NiCr_2O_4$	3.6	—	21.3	—	—	33.4	—	—	121	—	—	—	—
$MgCr_2O_4$	15.5	—	3.6	—	—	7.0	—	—	64	—	—	—	—

TABLE 5

Turnover Frequency (TOF) for Propene Formation in the Nickel Contained Spinels

Catalyst	Contributions of crystal faces (100)	(110)	(111)	Surface Ni concentration at. nm^{-2}	TOF $\times 10^3$ C_3H_6 molecules (at. Ni)$^{-1}$ s^{-1} 673 K	723 K	773 K
$Ni_{0.1}Mg_{0.9}Al_2O_4$	0.35	0.01	0.64	0.334	0.38	0.96	2.84
$Ni_{0.5}Mg_{0.5}Al_2O_4$	0.37	0.10	0.53	1.82	0.52	1.84	3.72
$NiAl_2O_4$	0.35	0.24	0.40	4.45	0.70	1.60	3.32
$NiCr_2O_4$	0.33	0.33	0.33	3.3	—	3.88	—

nonselective paths of oxidation—as has been claimed for other oxide systems (35). Further studies, now in course, are necessary to elucidate this problem.

The activation energy of steps 1 and 3 decrease with the increase in the Ni content, suggesting modification of the active centers for these steps. One may speculate that this modification consists in changing the electron density around oxygen atoms surrounding the nickel cations to facilitate the hydrogen abstraction from a propane molecule (a rate determining step in the selective oxidation reactions (35)) and/or the oxygen abstraction from the solids involved in the formation of carbon oxides.

On the other hand, the activation energy for the consecutive propene combustion increases with the Ni content, implying that a propene molecule is more strongly bound to the surface when Mg ions are being replaced by Ni ions. This may be due to stronger interaction of an olefinic molecule by donation of π electrons in the case of Ni (a transition metal ion with unfilled d orbitals) than in the case of Mg ions.

Table 5 lists TOF values for the propene formation (TOF is the number of propene molecules formed in one second per one surface Ni atom) on the NiMgAl spinels (after subtraction of the activity of $MgAl_2O_4$) and compares them with that for $NiCr_2O_4$. The TOF values were calculated from the initial rate of propene formation, obtained from the data at low conversions (<5%) by extrapolation. The number of Ni ions on the catalyst surface (column 5) was calculated taking into account the contributions of the most probable crystal faces to the total surface area of the spinels (columns 2–4). Fractions of various crystal faces were obtained with the Curie–Wulff construction, assuming the equilibrium shape of the crystal as reviewed in Refs. (11, 25). The conditions of preparation of the samples (high temperature and long time of heating) seem to justify this assumption. The TOF values at a given reaction temperature for the NiMgAl spinels are very close for $Ni_{0.5}Mg_{0.5}Al_2O_4$ and $NiAl_2O_4$ and are lower (particularly at lower reaction temperatures) for the spinel of the smallest Ni content, $Ni_{0.1}Mg_{0.9}Al_2O_4$. It should be, however, observed that for the latter compound the measured activity (the amount of propene formed) is small and only slightly different from that of $MgAl_2O_4$, so that the error in the evaluation of TOF can be high. The differences between the TOF values of the three NiMgAl spinels become smaller for higher reaction temperatures at which the overall activity is higher and hence the error in estimation of catalytic data is smaller. The standard error of the mean of the TOF values for the three spinels is 17% at 673 K and 8% at 773 K. $NiCr_2O_4$ shows much higher values of TOF as compared with the NiAl spinels.

The data obtained imply higher activity and lower selectivity in the ODH of propane of the Ni ions in the tetrahedral environment inherent in the $NiCr_2O_4$ spinel, as compared to the octahedral coordination in $NiAl_2O_4$. This is in keeping with the general rule stating that ions in an environment with a low CN are more apt to form a bond with a reacting molecule (an additional ligand) in the chemisorption process involved in a catalytic transformation than the ions of high CN. Higher activity of oxide catalysts in which metal ions acting as active centers are present in tetrahedral coordination as compared with octahedral has been reported for oxidation of CO to CO_2 on CuCr, CuFe, and CuRh spinels (40). In the ODH of propane on systems containing isolated VO_x groups dispersed on different supports, high selectivity and activity of the tetrahedral vanadium was observed (41, 42).

Another reason (besides the Ni coordination) for the higher activity and lower selectivity of the Cr-containing compounds may be the lower oxygen cation's bonding energy as compared with the NiMgAl spinels, as deduced from the calculations with the CMSS model. It is generally recognized that the oxide systems of low Me–O bond energy show low selectivity to partial oxidation products in the oxidation reactions, the loosely bound and mobile oxygen ions attacking an organic molecule at different carbon atoms and forming easily carbon oxides (35).

CONCLUSIONS

1. The NiMgAl and NiCr spinels are active and selective catalysts in oxidative dehydrogenation of propane.

2. In the $Ni_xMg_{1-x}Al_2O_4$ system the activity and selectivity in the ODH of propane increase with the increase in the Ni content. It is suggested that the Ni–O centers

are active in oxidative dehydrogenation of propane to propene.

3. $NiCr_2O_4$ spinel shows higher activity and lower selectivity to propene (at comparable propane conversions) as compared with the NiMgAl spinels. The comparison of the catalytic behavior of $MgCr_2O_4$ and $NiCr_2O_4$ with that of $MgAl_2O_4$ suggests that Cr–O centers in the spinel structure also participate (though to the smaller extent than Ni) in the propane–oxygen reactions.

4. The calculations with the CMSS model of the oxygen cation's bond energy show that oxygen ions in the Cr-containing spinels are less strongly bound than in the MgAl systems.

5. It is suggested that the differences in the activity and selectivity observed for the NiMgAl and NiCr spinels may be due to different coordination of Ni ions (confirmed by the XPS measurements): octahedral in NiMgAl and tetrahedral in NiCr systems. The higher activity and lower selectivity of the NiCr spinels may be also due to the lower oxygen cation's bond energy in these systems.

REFERENCES

1. Mazzocchia, C., Aboumrad, C., Diagne, C., Tempesti, E., Herrman, J. M., and Thomas, G., *Catal. Lett.* **10**, 181 (1991).
2. Mazzocchia, C., Tempesti, E., and Aboumrad, C., US Patent 5,086,032 (1992).
3. Yoon, Y. S., Fujikawa, N., Ueda, W., Moro-oka, Y., and Lee, K. W., *Catal. Today* **24**, 327 (1995).
4. Stern, D. L., and Grasselli, R. K., *J. Catal.* **167**, 550 (1997).
5. Takita, Y., Kurosaki, K., Mizuhara, Y., and Tshihara, T., *Chem. Lett.* 335 (1993).
6. Takita, Y., Sano, K., Kurosaki, K., Kawata, N., Nishiguchi, H., Ito, M., and Ishihara, T., *Appl. Catal. A* **167**, 49 (1998).
7. Moriceau, P., Grzybowska, B., and Barbaux, Y., *Polish J. Chem*. **72**, 910 (1998).
8. Ziółkowski, J., *J. Solid State Chem*. **57**, 269 (1985).
9. Ziółkowski, J., and Dziembaj, L., *J. Solid State Chem*. **57**, 291 (1985).
10. Ziółkowski, J., *J. Catal.* **100**, 45 (1986).
11. Ziółkowski, J., *Surf. Sci.* **209**, 536 (1989).
12. Scofield, J. H., *J. Electron Spectrosc.* **8**, 129 (1976).
13. Lenglet, M., D'Huysser, A., Arsène, J., Bonnelle, J. P., and Jørgensen, C. K., *J. Phys. C* **19**, L363 (1986).
14. Lenglet, M., D'Huysser, A., and Jørgensen, C. K., *Inorg. Chim. Acta* **133**, 61 (1987).
15. Lenglet, M., and D'Huysser, A., *C. R. Acad. Sci. Paris II* **310**, 483 (1990).
16. Venezia, A. M., Bertoncello, R., and Deganello, G., *Surf. Interface Anal.* **23**, 239 (1995).
17. Hill, R. J., Craig, J. M., and Gibbs, G. V., *Phys. Chem. Miner.* **4**, 317 (1979).
18. Inaba, H., Yagi , H., and Naito, K., *J. Solid State Chem*. **64**, 67 (1986).
19. Atanasov, M., Kesper, U., Ramakrishna, B. L., and Reinen, D., *J. Solid State Chem*. **105**, 1 (1993).
20. Bertaut, F., *C. R. Acad. Sci. Paris* **230**, 213 (1950).
21. Greenwald, S., Pickart, S. J., and Granis, F. H., *J. Chem. Phys.* **22**, 1597 (1954).
22. Davies, M. J., Parker, S. C., and Watson, G. W., *J. Mater. Chem*. **4**, 813 (1994).
23. Binks, D. J., Grimes, R. W., Rohl, A. L., and Gay, D. H., *J. Mater. Sci.* **31**, 1152 (1996).
24. Ziółkowski, J., Barbaux, Y., *J. Molec. Catal.* **67**, 199 (1991).
25. Ziółkowski, J., Bordes, E., and Courtine, P., *J. Catal.* **122**, 126 (1990).
26. Ziółkowski, J., *J. Solid State Chem*. **121**, 388 (1996).
27. Chaar, M. A., Patel, D., and Kung, H. H., *J. Catal.* **109**, 463 (1988).
28. Siew Hew Sam, D., Soenen, V., and Volta, J. C., *J. Catal.* **123**, 417 (1990).
29. Michalakos, P. M., Kung, M. C., Jahan, I., and Kung, H. H., *J. Catal.* **140**, 226 (1993).
30. Słoczyński, J., Grabowski, R., Wcisło, K., and Grzybowska-Świerkosz, B., *Polish J. Chem*. **71**, 1585 (1997).
31. Andersson, S. L. T., *Appl. Catal. A: General* **112**, 209 (1994).
32. Boisdron, N., Monnier, A., Jalowiecki-Duhamel, L., and Barbaux, Y., *J. Chem. Soc., Faraday Trans.* **91**, 2899 (1995).
33. Stern, D. L., and Grasseli, R. K., *J. Catal.* **167**, 560 (1997).
34. Słoczyński, J., *Appl. Catal. A: General* **146**, 401 (1996).
35. Bielański, A., and Haber, J., *in* "Oxygen in Catalysis." Marcel Dekker, New York, 1991, and references therein.
36. Grabowski, R., Grzybowska, B., Samson, K., Słoczyński, J., and Wcisło, K., *React. Kin. Catal. Lett.* **57**, 127 (1996).
37. Grabowski, R., Grzybowska, B., Słoczyński, J., and Wcisło, K., *Appl. Catal. A* **144**, 335 (1996).
38. Moriceau, P., Grzybowska, B., Barbaux, Y., Wrobel, G., and Hecquet, G., *Appl. Catal. A* **168**, 269 (1998).
39. Grzybowska, B., Słoczyński, J., Grabowski, R., Wcisło, K., Kozłowska, A., Stoch, J., and Zieliński, J., *J. Catal.* **178**, 687 (1998).
40. Ghose, J., and Murthy, K. S. R. C., *J. Catal.* **162**, 359 (1996).
41. Corma, A., López-Nieto, J. M., Parades, N., Pérez, M., Shen, Y., Cao, H., and Suib, S. L., *Stud. Surf. Sci. Catal.* **72**, 213 (1992).
42. Concepcion, P., López-Nieto, J. M., and Pérez-Pariente, J., *Catal. Lett.* **19**, 333 (1993).